

Analysis of proton MRSI metabolites with improved tissue segmentation at 7T

Yoojin Lee¹, Tae Kim¹, Tiejun Zhao², Julie W. Pan¹, and Hoby P. Hetherington¹

¹Department of Radiology, University of Pittsburgh, Pittsburgh, Pennsylvania, United States, ²Siemens Medical Solution USA, INC., Siemens MediCare USA, Pittsburgh, Pennsylvania, United States

Target audience: Researchers in spectroscopic imaging

Purpose: Analysis of brain MRSI data for neurological disorders requires accurate tissue segmentation¹. This is particularly relevant for ultra-high field where SNR and spectral resolution are improved although B_1 homogeneity for transmission and reception is known to be challenging. Recently, a simple technique was developed to reduce signal intensity variations induced by B_1 inhomogeneity, dividing high-resolution 3D T_1 -weighted magnetization-prepared rapid acquisition with gradient echo (MPRAGE) images by gradient-echo (GRE) images². This technique also removes proton density and T_2^* contrast from T_1 -weighted signal and results in much purer T_1 contrast data. In this study, we applied this approach to improve tissue segmentation at 7 T for more precise metabolic analysis for MRSI.

Methods: Data from three healthy volunteers and one tumor patient were acquired on a 7T Siemens scanner using an 8 channel inductively decoupled 1H transceiver array. A 28 channel shim insert coil with a 38cm ID consisting of Z0, all 2nd-4th degree shims and partial 5th and 6th degree shims with 5A shim supplies (Resonance Research Inc.) was used for higher degree/order B_0 shimming. For the MRSI data acquisition, two B_1^+ distributions were optimized for homogeneous excitation of the brain and to selectively suppress extracerebral tissues³. MRSI data were acquired using TE/TR = 40/1500 ms, FOV = 200×200mm², matrix size = 24×24, and slice thickness = 10 mm (voxel size = 8.3×8.3×10mm³). For reconstruction of metabolite SI data, 3DFFT including 2D Hanning filter along spatial axes and 4-Hz Gaussian filter along spectral axis was performed and a convolution difference using a line broadening of 100 Hz was applied. The high-resolution MPRAGE images were acquired for tissue segmentation with TE/TR/TI = 1.8/3000/1200 ms, flip angle = 8°, 0.9 mm isotropic voxel, GRAPPA = 2, acquisition time = 5 min 21 sec. To reduce residual signal variation arising from B_1 inhomogeneity in MPRAGE images, additional GRE images were acquired by eliminating inversion pulses and reducing flip angle to 2° (acquisition time = 1 min 24 sec). The conventional MPRAGE images were divided by the GRE images and the resulting images segmented to GM, WM, and cerebrospinal fluid (CSF). The percent GM from each MRSI voxel was calculated after including point-spread function (PSF) corresponding to the acquired MRSI data. Spectral data were analyzed in the spectral domain. The data set of percent GM and Cr/NAA from all healthy subjects was used for linear regression analysis. The tumor patient suffered from a possible recurrent glioblastoma centrally located in the right brain; this data was processed equivalently and compared with the linear regression results from healthy subject data.

Results and Discussion: Figure 1 shows that both the conventional MPRAGE and GRE images have the typical decrease signal in the center region of the brain mainly due to the B_1 inhomogeneity. This effect is minimized in normalized images (MPRAGE/GRE, Fig. 1c), resulting in much more consistent contrast. Figure 2a,b show the scout and spectra from the tumor patient (green box shows region of all spectra). Figure 2c shows the linear regression from three healthy subjects (black line is the calculated regression which is highly significant at $R=0.66$; blue lines are 99% confidence on the regression). The green lines show the 99% prediction interval for an additional point. The voxels from the tumor patient are also shown in Fig. 2c (red). Among them, the voxels that lie outside the 99% prediction interval were considered to be abnormal. The relatively large number of the voxels was determined to be abnormal for the tumor patient. One likely explanation is the variation in Cr/NAA between different gray matter regions. In order to account for this, further segmentation into different regions of GM is necessary. We performed cortical parcellation using conventional MPRAGE vs. normalized images using Freesurfer⁴, and found more reliable parcellation results from normalized image, showing clearer segmentation of thalamus (red arrows) and hippocampus (black arrows) (Fig. 3). In conclusion we show that normalization of MPRAGE images at 7T improves segmentation and parcellation, and is likely to be useful to more accurate analysis of MRSI data.

References: 1. Hetherington HP, Pan JW, et al. Quantitative 1H spectroscopic imaging of human brain at 4.1T using image segmentation. Magn Reson Med 1996;36:21–29. 2. Van de Moortele PF, et al. T1 weighted brain images at 7T unbiased for Proton Density, T_2^* contrast and RF coil receive B_1 sensitivity with simultaneous vessel visualization. Neuroimage 2009;46:432–446. 3. Hetherington HP, Avdieievich NI, Kuznetsov AM, Pan JW. RF shimming for spectroscopic localization in the human brain at 7 T. Magn Reson Med 2009;63:9–19. 4. Fischl B, et al. Whole brain segmentation: automated labeling of neuroanatomical structures in the human brain. Neuron 2002;33:341–355.

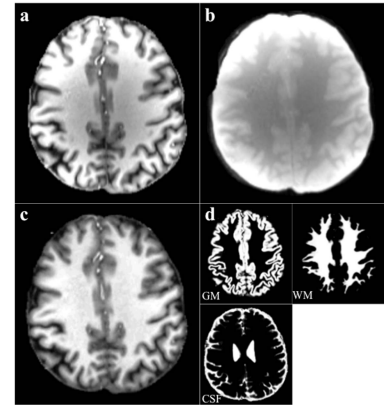


Fig. 1. (a) Conventional MPRAGE image. (b) GRE image. (c) MPRAGE/GRE ratio image. (d) Segmentation results of (c).

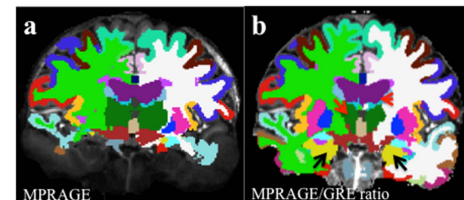
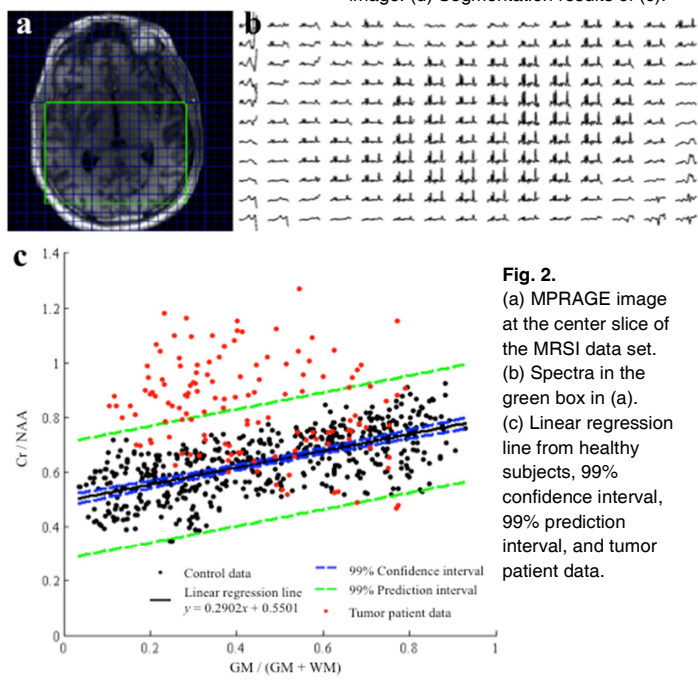


Fig. 3.
 Parcellation results with (a) conventional MPRAGE images and (b) MPRAGE/GRE ratio images.